

# BENA435, a new cell-permeant photoactivated green fluorescent DNA probe

Alexandra Erve, Yasmina Saudi, Sylvie Thiro<sup>1</sup>, Corinne Guetta-Landras<sup>1</sup>,  
Jean-Claude Florent<sup>1</sup>, Chi-Hung Nguyen<sup>1</sup>, David S. Grierson<sup>1</sup>  
and Andrei V. Popov\*

Inserm, U366, DRDC/CS, CEA-Grenoble, 17, rue des Martyrs, F-38054, Grenoble, cedex 9 France and  
<sup>1</sup>Laboratoire de Pharmacochimie, UMR176 CNRS-Institut Curie, Institut Curie Section de Recherche,  
Batiment 110, Centre Universitaire, 91405 Orsay, France

Received October 12, 2005; Revised January 27, 2006; Accepted February 12, 2006

## ABSTRACT

*N'*-(2,8-Dimethoxy-12-methyl-dibenzo [c,h] [1,5] naphthyridin-6-yl)-*N,N*-dimethyl-propane-1,3-diamine (BENA435) is a new cell-membrane permeant DNA dye with absorption/emission maxima in complex with DNA at 435 and 484 nm. This new reagent is unrelated to known DNA dyes, and shows a distinct preference to bind double-stranded DNA over RNA. Hydrodynamic studies suggest that BENA435 intercalates between the opposite DNA strands. BENA435 fluoresces much stronger when bound to dA/dT rather than dG/dC homopolymers. We evaluated 14 related dibenzonaphthyridine derivatives and found BENA435 to be superior in its *in vivo* DNA-binding properties. Molecular modelling was used to develop a model of BENA435 intercalation between base pairs of a DNA helix. BENA435 fluorescence in the nuclei of cells increases upon illumination, suggesting photoactivation. BENA435 represents thus the first known cell-permeant photoactivated DNA-binding dye.

## INTRODUCTION

Nucleic acid-binding fluorescent compounds are widely used for DNA visualization, purification and quantification (1). Since the 1950s a variety of DNA and RNA non-covalently binding probes have been discovered. They can be classified according to their molecular structure, the class of nucleic acids they bind to, and their mode of binding. The most frequently used fluorescent dyes (Hoechst, DAPI and ethidium bromide) bind strongly and preferentially to double-stranded

DNA (dsDNA), while others (such as the SYTO dyes) stain all types of nucleic acids depending on the conditions (1). These properties correlate well with the molecular structures of these reagents. For example, ethidium bromide and propidium iodide intercalate into dsDNA (2), whereas the cationic dyes Hoechst and DAPI interact with the minor groove of dsDNA, showing a net preference for dA/dT rich sequences (3,4). Interestingly, certain DNA markers show both types of binding, depending on their concentration relative to nucleic acids (5).

Experimentation with live cells is dependent on the possibility to illuminate cells for relatively long periods of time without inflicting damage. However, most of the traditional cell-permeant DNA-binding dyes used in cell biology (DAPI, Hoechst 33342 or 33258) require illumination with light in the ultraviolet (UV, 200–400 nm) part of the spectrum. At these wavelengths extensive photodamage occurs, due, amongst other things, to formation of free radicals, and to cross-links in DNA and/or DNA-associated proteins (6,7). These events are followed by failure to replicate DNA and/or failure to enter (8) and accomplish mitosis. This ultimately leads to cell cycle arrest and death (9). Both ethidium bromide and propidium iodide can be excited at longer than UV wavelengths. However, propidium bromide does not penetrate into cells, and ethidium bromide intercalates into the DNA of living mammalian cells to only a very limited extent (10). There is thus a need to develop new fluorescent DNA probes for live-cell video microscopy and cell sorting which are (i) cell membrane-permeant and non-toxic; (ii) excited at longer than UV wavelengths; and (iii) stable over long periods of illumination.

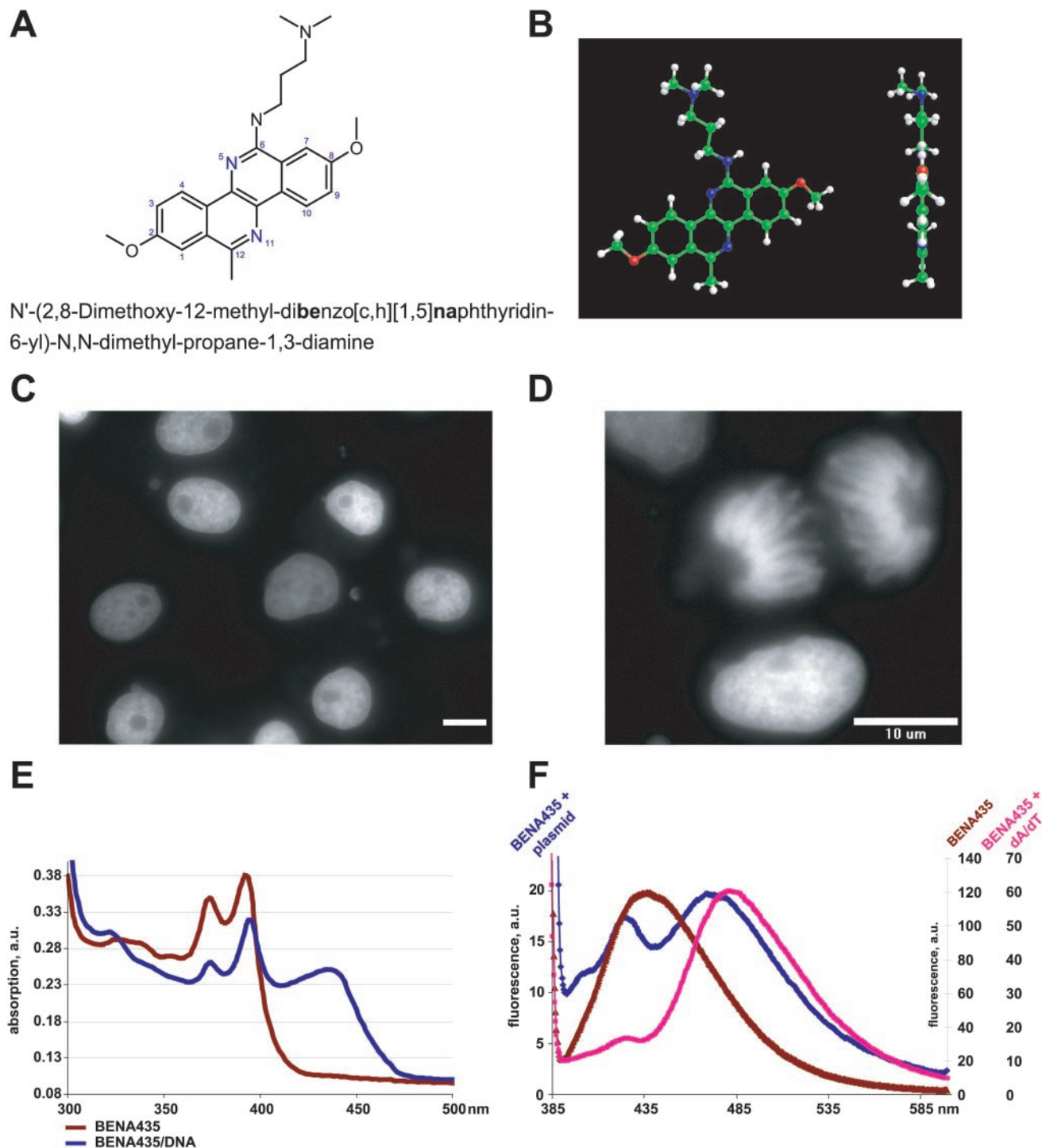
In this work we describe the discovery of *N'*-(2,8-dimethoxy-12-methyl-dibenzo [c,h][1,5]naphthyridin-6-yl)-*N,N*-dimethyl-propane-1,3-diamine (BENA435) (Figure 1A),

\*To whom correspondence should be addressed. Tel: +33 4 38 78 54 82; Fax: +33 4 38 78 50 57; Email: andrei.popov@cea.fr

The authors wish it to be known that, in their opinion, the first two authors should be regarded as joint First Authors

© The Author 2006. Published by Oxford University Press. All rights reserved.

The online version of this article has been published under an open access model. Users are entitled to use, reproduce, disseminate, or display the open access version of this article for non-commercial purposes provided that: the original authorship is properly and fully attributed; the Journal and Oxford University Press are attributed as the original place of publication with the correct citation details given; if an article is subsequently reproduced or disseminated not in its entirety but only in part or as a derivative work this must be clearly indicated. For commercial re-use, please contact journals.permissions@oxfordjournals.org



N'-(2,8-Dimethoxy-12-methyl-dibenzo[c,h][1,5]naphthyridin-6-yl)-N,N-dimethyl-propane-1,3-diamine

**Figure 1.** BENA435 is a new fluorescent DNA dye. (A) Molecular structure and the name of BENA435. (B) The 3D model of BENA435 showing a flat structure in perspective and orthogonal projections. (C) Nuclei of interphase cells stained *in vivo* with BENA435. *Xenopus* XL 177 cells were incubated in the presence of 5  $\mu$ M BENA435 and illuminated using a standard Alexa488/FITC filter set. (D) Mitotic chromosomes (anaphase) stained *in vivo* with BENA435. (E) Absorption spectra of free and DNA-bound BENA435 at 25  $\mu$ M mixed with plasmid DNA at bp/dye ratio 8. (F) Emission spectra of free and DNA-bound 1  $\mu$ M BENA435. Note that upon DNA binding the peak of free BENA435 at 438 nm decreases and shifts to 426 nm, while a new peak evolves around 472–484 nm. Plasmid DNA and dA/dT homopolymer were used at bp/dye ratio 20. In both cases BENA435 was excited at 373 nm to allow the visualization of the free BENA435 fluorescence. Size bar in (C) and (D), 10  $\mu$ m.

a new dsDNA-binding cell-permeant fluorescent dye. As its name suggests, this compound in complex with dsDNA shows an absorption maximum at 435 nm, while its emission peaks are at 484 nm making it possible to visualize DNA using a

standard Alexa488/FITC filter set. BENA435 can interact with DNA through intercalation and it fluoresces preferentially when bound to dA/dT rather than to dG/dC nucleic acids polymers. Evaluation of fourteen BENA435-related compounds

allowed us to correlate their structures with their fluorescent properties. Using BENA435 for DNA quantification in cells it was determined that the total fluorescence of BENA435-stained nuclei is proportional to their DNA content, a feature useful for cell-cycle monitoring both *in vivo* and for fixed cells. To our knowledge, BENA435 is the first long wavelength non-toxic photoactivated fluorescent DNA dye reported for use as a DNA probe in cell biology.

## MATERIALS AND METHODS

### Curie-CNRS compound library and BENA435 synthesis

A highly diverse proprietary library of 4080 compounds, corresponding to molecules synthesized by the Pharmacochimistry Laboratory at Institut Curie (UMR 176 CNRS-IC) was used as the compound set in the screening assays ('Chimiothèque Nationale', <http://chimiotheque-nationale.enscm.fr>). Library components were formed in 96-well microplates in anhydrous DMSO at 10 mM and stored at +4°C in the dark. All manipulations were carried out taking care to protect the compounds from excessive light. The synthesis of BENA435 and the related 6-amino substituted dibenzonaphthyridines **4**, **12**, **13** have been already described in Ref. (11). Additional information on BENA435 and related molecules **1**, **2**, **3**, **5**, **6**, **7**, **8**, **9**, **10**, **11** and **14** is presented in the Supplementary Data.

### Cell culture and screening

In this study three different types of cells were used: *Xenopus* epithelial cell line XL177 (12), mouse fibroblasts and primary human skin fibroblasts. XL177 cells were grown at 20°C in 60% Leibowitz-15 medium, supplemented with antibiotics, 10% fetal calf serum (FCS) and 10 mM HEPES, pH 7.2 with addition of 0.7 mg/ml G418. Cells were plated into glass-bottom 96-well plates (Greiner, Germany) and left to spread for 24 h before being incubated in the presence of the test compounds (at 25 or 50 µM final concentration) for another 20–24 h. Mouse and human fibroblasts were grown in DMEM with antibiotics and 10% FCS at 37°C in the presence of 5% CO<sub>2</sub>. We observed the cells using a Zeiss Axiovert 200M microscope with a 40× oil immersion objective and a standard Alexa488/FITC filter (XF100–2; Ex475AF40/Em535AF45/Dichroic505; Omega). For the *in vivo* tests of BENA435-like compounds, the molecules were added to cell culture medium at 10 µM final concentration and incubated with cells 10–60 min (up to 24 h) prior to scoring.

### Reagents

Plasmid dsDNA was purified using a Qiagen Maxiprep kit and used in the supercoiled form for absorption and fluorescence studies. *Escherichia coli* total RNA was bought from Ambion, dA/dT and dG/dC homopolymers were purchased from Amersham Biosciences. Calf thymus (CT) high-molecular weight DNA and Hoechst 33258 were obtained from Sigma-Aldrich. Ethidium bromide was purchased from Amresco.

### Spectrometry and fluorimetry

Spectrometry and fluorimetry were performed using a SpectraMax384 (Molecular Devices) and a Luminescence

Spectrometer LS50B (Perkin Elmer). Fluorescence emission of BENA435 in complex with DNA and RNA was measured in 50 mM Na phosphate buffer, pH 7.2 at room temperature. Before use, total *E. coli* RNA was heated to 100°C for 1 min and immediately transferred on ice for 5 min before mixing with BENA435 solution. All measurements were carried out at room temperature (20–23°C) in solutions protected from light and incubated for ~10–15 min after dilution. The units of b/dye and bp/dye are defined as moles of RNA bases or DNA base pairs per mole of dye. Quantum yield was measured using quinine sulphate as standard as described in Ref. (13) using FLUOROMAX-3 Spex Spectrofluorometer (HORIBA) and UVIKON XL Spectrophotometer (SECOMAM).

### Viscometry

CT DNA was dissolved in 50 mM Na-phosphate buffer, pH 7.2, to a concentration of 0.1 or 0.5 mM relative to base pairs as described in the legend for Figure 3A and B. DNA solution was allowed to run through a custom-made capillary viscometer and the time necessary for the meniscus to pass a certain distance was measured using a stopwatch. All experiments were performed at 23°C. Viscosity values were calculated using the equation  $\eta = (t - t_0)/t_0$ , where  $t$  is the flow time of DNA solution (with or without dye), and  $t_0$  is the flow time of Na-phosphate buffer alone. For each sample flow times were measured three to five times. Viscosity of DNA solutions with dyes were calculated as  $(\eta/\eta_0)^{1/3}$ , where  $\eta_0$  and  $\eta$  are relative viscosities of the CT DNA solution in the absence and presence of the dye, respectively (14). Average viscosity values and SEM were determined using  $(\eta/\eta_0)^{1/3}$  values calculated for each time flow measurement.

### Measuring nuclear fluorescence in live cells stained with BENA435

BENA435 at 5 µM was added directly into the cell medium 10 min before observation in an inverted microscope Zeiss Axiovert 200M with a 100 W mercury lamp. Time-lapse images were acquired using CoolSnap HQ (Photometrics, Inc.) black and white camera driven by the Metamorph software (Universal Imaging). All experiments were carried out using 40× or 63× (Figure 1C and D) oil immersion Apochromat Zeiss objectives. To measure the fluorescence intensities an oval region was drawn inside of each nucleus using Metamorph software and integrated intensities (nuclear surface multiplied by the average pixel value) were logged for each image.

### Measuring nuclear fluorescence in fixed cells stained with BENA435

Primary human skin fibroblasts were grown on poly-D-lysine-coated glass coverslips and fixed in cold (–20°C) anhydrous methanol for 15 min. Samples were re-hydrated in phosphate-buffered saline (PBS) (150 mM NaCl, 20 mM Na-phosphate, pH 7.2), rinsed with 10% PBS (diluted with water) and stained with 120 µM BENA435 in 10% PBS for 15 min at room temperature in the dark. Samples were mounted, without washing, using the FluorSave™ mounting medium (Calbiochem) or Mowiol and analysed within 3 h. For image acquisition (Figure 5B and D) cells were illuminated continuously (open shutter) for 30 min using an Omega filter set XF100–2

(see above). Images were acquired at 10 s intervals and stored in a 16-bit format as a stack. Integrated intensities of nuclear fluorescence were measured as described above and logged for each of the 180 images. Fluorescence of each region at the last time point was taken as 100% and fluorescence intensities at the same region at previous time points (frames) were calculated using Microsoft Excel software.

### Spectral analysis of BENA435 fluorescence in live cells

BENA435 at 5  $\mu\text{M}$  final concentration was added to live 3T3 mouse cells in DMEM just before observation using a Leica TCS-SP2 laser-scanning confocal microscope. Cellular fluorescence was observed for 20 min under continuous excitation at 405 or 458 nm using the 'Lambda scanning' mode to record the emission spectra of BENA435.

### Molecular modelling

The 3D atomic coordinates of BENA435 in pdb format were obtained using web-based CORINA software (<http://www2.chemie.uni-erlangen.de/software/corina/corina.html>) (15). For computer-assisted molecular modelling we employed the ArgusLab software (16) which makes use of either AScore or the Lamarckian genetic algorithm (17) scoring functions to find the low-energy binding modes. For docking of BENA435 into dsDNA we used 3D molecular coordinates of a DNA dodecamer 5'-D(CpGpCpGpApApTpTpCpGpCpG)-3' crystallized with an Acridine-Peptide drug intercalated in an Aa/Tt Base Step [protein data bank PDB ID—1G3X (18)]. Prior to docking of BENA435, *N*( $\alpha$ )-(9-Acridinoyl)-Tetraarginine-Amide was removed from the complex with DNA and hydrogens were added to both BENA435 and DNA. Molecular graphics images were produced using the UCSF Chimera package from the Resource for Biocomputing, Visualization and Informatics at the University of California, San Francisco (19).

## RESULTS

### BENA435 stains interphase nuclei in live cells

During a visual phenotypic screen of the Curie-CNRS compound library on live *Xenopus* cells XL177 (using an Alexa488/FITC filter) it was found that BENA435 produced a bright green nuclear signal (Figure 1C). The signal appeared after 10–20 s illumination and was stable for many minutes thereafter (see below). The observed nuclear staining in cultured cells indicates that (i) the drug is cell-membrane permeant; (ii) non-toxic under standard cell culture conditions (up to 6 days in culture, data not shown); and (iii) stains DNA or chromatin proteins or is simply accumulated in the nucleus.

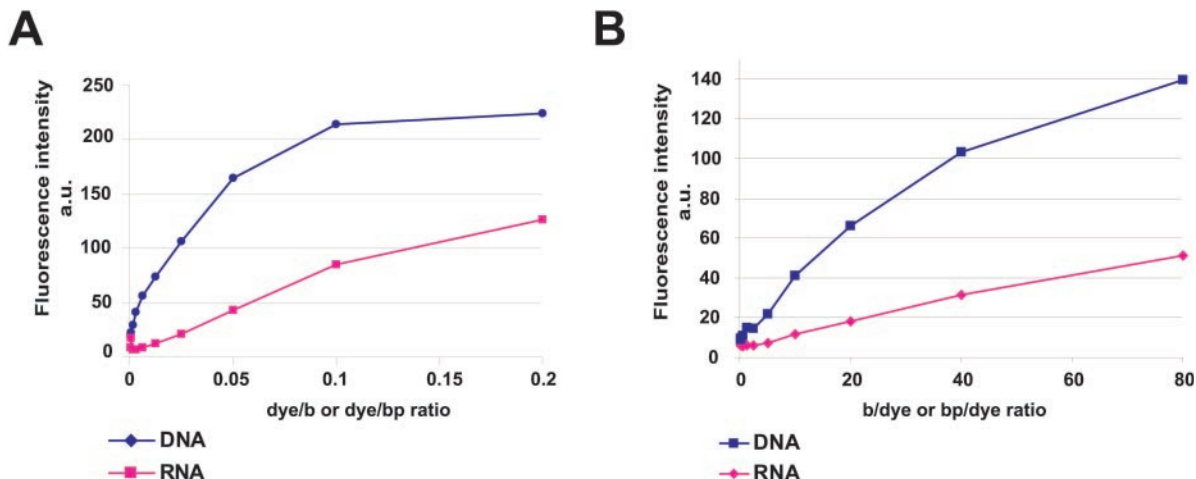
### Spectral characteristics of BENA435 change upon DNA binding

Nuclear staining *per se* does not prove that a dye binds to DNA, as it could simply accumulate in the nucleus. Although BENA435 also stains mitotic chromosomes (Figure 1D), theoretically it was possible that it binds specifically to DNA-associated proteins (e.g. histones) rather than to nucleic acids. To resolve this issue, the absorption and emission spectra of free BENA435 before and after addition of dsDNA were recorded. Free BENA435 shows a complex absorption profile

with maxima at 224, 245, 283, 326, 373 and 391 nm (Figure 1E shows the part of spectrum from 300 to 550 nm). Molar extinction coefficient of free BENA435 at 391 nm was measured at  $10\,800\text{ cm}^{-1}\text{ M}^{-1}$ . In the presence of ds plasmid DNA the absorption peaks of BENA435 at 373 and 391 nm decreased, and a new peak appeared with a maximum at 435 nm (Figure 1E). An overlay of the absorption spectra in complex with dsDNA at different base pairs per dye ratios gives a single isosbestic point at 398 nm (Supplementary Data). Free BENA435 fluoresces around 438 nm (the exact position of the peak depends on the excitation wavelength). Upon DNA binding the emission peak at 438 nm decreases and shows a hypsochromic shift to 426 nm. At the same time a new peak evolves with a maximum around 484 nm (Figure 1F). The exact maximum of fluorescence of BENA435/DNA complexes varies insignificantly as a function of the dye/bp ratio and/or base pairs composition of the nucleic acids. For example, as shown in Figure 1F, plasmid DNA at bp/dye ratio 40 gives a maximum at 472 nm, while in the presence of dA/dT homopolymers at the same bp/dye ratio BENA435 shows a maximum at 484 nm (see also below). When BENA435/dsDNA solutions are excited at different wavelengths ranging from 300 to 500 nm, we found that although the fluorescence intensity varies considerably (with maximum found when excited at 435 nm), the emission always shows a major peak of fluorescence around 484 nm and (for shorter excitation wavelengths 323, 348, 373 and 391) a shoulder at 420 nm (Supplementary Data). The quantum yield for BENA435 (excited at 435 nm) at 5  $\mu\text{M}$  in 50 mM Na-phosphate, pH 7.2, was determined to be 2.7% for free dye and 13.8% in admixture with 50  $\mu\text{M}$  CT DNA. These results show that BENA435 is a new DNA-binding fluorescent probe with excitation and emission in the blue/green part of the visible light spectrum.

### BENA435 binds preferentially to dsDNA compared with RNA

A number of known fluorescent dyes bind preferentially to dsDNA, while others, like the SYTO dyes bind similarly well to dsDNA, single-stranded DNA (ssDNA) and RNA (1). Knowing these properties is important to the design of experiments where one or another (or several) type(s) of nucleic acids may be present. To investigate the selectivity of BENA435 we compared fluorescence intensities at 484 nm of the dye incubated with ds plasmid DNA or heat-denatured *E.coli* RNA. For this, DNA or RNA at 50  $\mu\text{M}$  (relative to base or base pairs) was titrated with different amounts of BENA435. As shown in Figure 2A, at low dye/bp and dye/b ratios the emission strength of BENA435 was significantly higher (6-fold) when mixed with DNA rather than RNA. At higher dye/b or dye/bp ratio the difference was smaller [1.8-fold at dye/b(bp) ratio 0.2], meaning that elevated amounts of dye could saturate both types of nucleic acids. We then performed the experiment in the opposite sense, i.e. titrating a fixed amount of BENA435 at 1  $\mu\text{M}$  with increasing amounts of DNA and RNA. As demonstrated in Figure 2B, the fluorescence of BENA435 mixed with dsDNA was, once again, significantly (2.5–3.6) higher compared with RNA at the same b(bp)/dye ratios. Moreover, fixed amounts of BENA435 could be saturated by increasing amounts of dsDNA at  $\sim 30$  bp/dye ratio, but not with increasing quantities



**Figure 2.** BENA435 binds preferentially to dsDNA rather than to RNA. (A) Fluorescence emission values of different amounts of BENA435 mixed with 50  $\mu$ M dsDNA or RNA. (B) Fluorescence emission values of 1  $\mu$ M BENA435 titrated with dsDNA and RNA.

of RNA (up to 250 b/dye ratio; Supplementary Data). Taken together, these results show that BENA435 has a high selectivity for dsDNA over RNA explaining the exclusive nuclear staining observed in cells (Figure 1C).

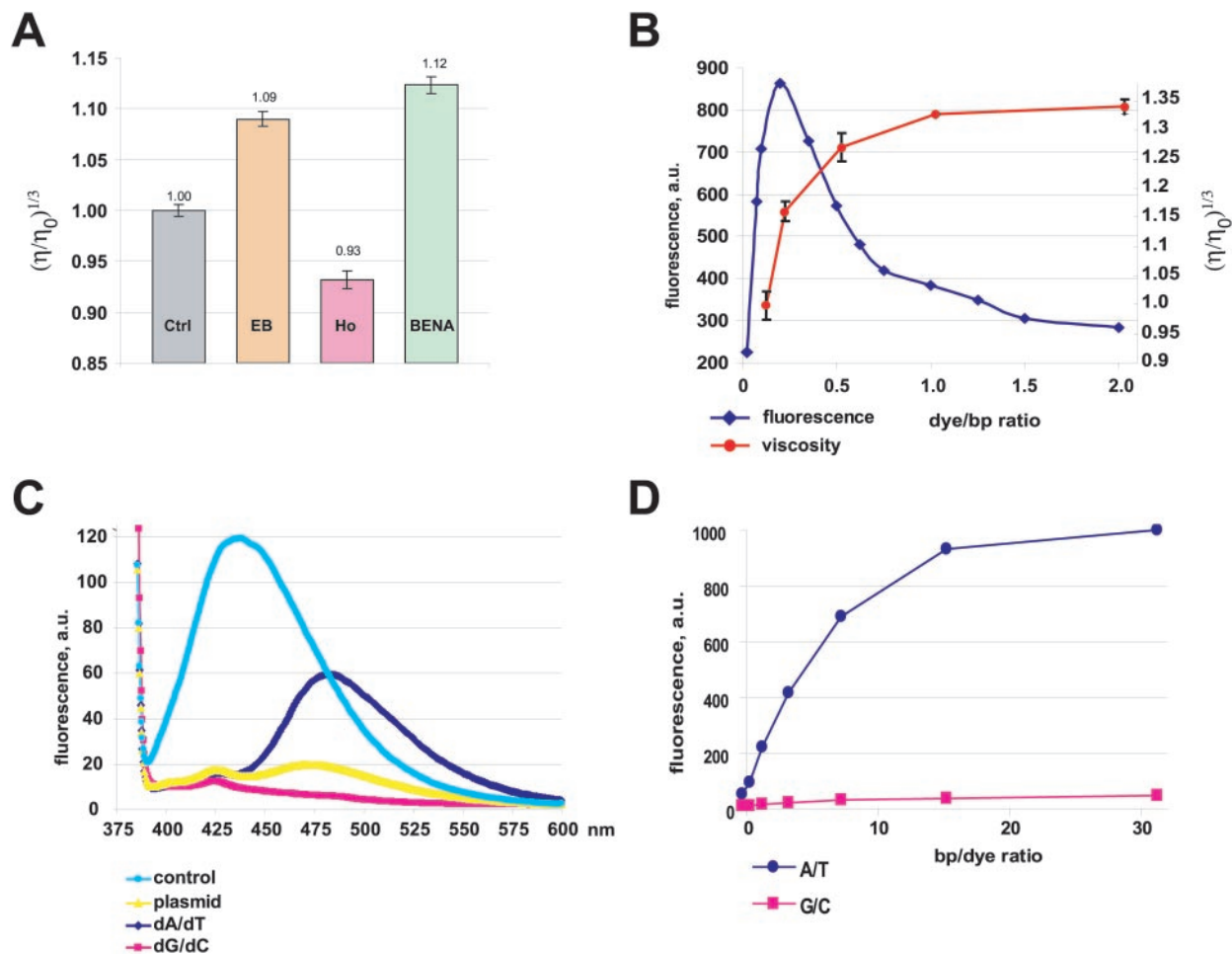
#### Hydrodynamic studies of BENA435 show that it can intercalate between DNA strands.

DNA-binding dyes interact with dsDNA by intercalation or external binding, or both. In order to determine the mechanism of BENA435 binding to dsDNA we performed hydrodynamic studies. This approach is based on the observation that intercalating molecules increase the length of DNA fragments and, consequently, enhance the viscosity of DNA solutions (14,20). For this experiment we compared BENA435 with the known DNA intercalator ethidium bromide and with the external minor groove binder Hoechst 33258. CT DNA at 0.5 mM was mixed with drugs at 0.1 mM concentration (0.2 dye/bp ratio) and used for viscometry measurements. As shown in Figure 3A, BENA435 behaves in the same way as ethidium bromide, increasing the viscosity of the DNA solution. In contrast, as described previously (5), the viscosity was found to decrease slightly for Hoechst 33258.

We then asked ourselves whether the increase in viscosity is equally matched by the increase in fluorescence intensity. To answer this question CT DNA at 0.1 mM (bp) was mixed with increasing amounts of BENA435 and viscosity measurements were performed as above. The viscosity of the DNA/BENA435 solutions increased up to a dye/bp ratio 1 (Figure 3B). To correlate the increase in viscosity with fluorescence we measured fluorescence intensities at 484 nm of the BENA435/DNA solutions used for the viscosity measurements. The maximal fluorescence intensity was reached at dye/bp ratio 0.2, after which it quickly diminished (Figure 3B). Since the viscosity of the DNA/BENA435 solutions continues to increase up to the dye/bp ratio 1, the latter result suggests a 'quenching' effect (21). In conclusion, hydrodynamic studies show that BENA435 can intercalate into dsDNA.

#### BENA435 fluoresces preferentially when bound to dA/dT rather than dG/dC DNA tracts

Many intercalating dyes and minor groove-binding DNA dyes can interact differently with dA/dT or dG/dC DNA tracts. More interestingly, even for those dyes that bind similarly well to dA/dT and dG/dC sequences, the nature of the nucleotides can affect the intensity of fluorescence (22). To investigate the properties of BENA435 when bound to different DNA tracts, we examined its fluorescence in admixture with an excess of plasmid DNA and either dA/dT or dG/dC homopolymers. Figure 3C shows that upon plasmid DNA binding BENA435 develops a peak at 484 nm, while the peak at 438 nm decreases significantly. The peak at 484 nm was much more pronounced when plasmid DNA was replaced by the dA/dT homopolymers (see also Figure 1F). Surprisingly, in admixture with dG/dC homopolymer, the intensity of BENA435 fluorescence at 484 nm was 9.5-fold lower compared with BENA435-dA/dT. This effect cannot be explained by the lack of binding to DNA, because the peak of fluorescence at 438 nm is sharply diminished (12.7-fold reduction; the peak also shifts to 426 nm). In Figure 3C the graphs show emission spectra upon excitation at 371 nm to allow plotting the emission of free BENA435. Similar results were obtained when exciting DNA/BENA435 complexes at 391 and 435 nm (data not shown). We quantified the difference in fluorescence of BENA435 when bound to dA/dT and dG/dC homopolymers at different dye per base pairs ratios and found that the difference was 23-fold at dye/bp ratio 8 (Figure 3D). Interestingly, the absorbance spectra of BENA435 bound to dG/dC and dA/dT homopolymers are very similar up to a dye/bp ratio 1. At higher bp/dye ratios BENA435-dG/dC absorption at 435 nm is  $\sim$ 30% superior than that of BENA435-dA/dT (Supplementary Data), suggesting that BENA435 binds similarly well to both DNAs and the difference in fluorescence intensity does not reflect the lack of binding to dG/dC tracts. Taken together, these results suggest that BENA435 binds similarly well to both dA/dT and dG/dC tracts but fluoresce preferentially when complexed with dA/dT sequences.



**Figure 3.** BENA435 increases the viscosity of DNA solutions and fluoresces preferentially when bound to dA/dT rather than dG/dC DNA tracts. (A) Relative viscosities  $[(\eta/\eta_0)^{1/3}]$  of 0.5 mM CT DNA in the absence (Ctrl) or presence of different dyes at 0.1 mM concentration: ethidium bromide (EB), Hoechst 33258 (Ho) and BENA435. (B) Relative viscosities of CT DNA solutions in the presence of different amounts of BENA435 (red curve; y-axis on the right-hand side). Blue curve shows fluorescence intensity of the same DNA/BENA435 solutions used for viscosity measurements (y-axis on the left-hand side). (C) Fluorescence spectra of 1  $\mu$ M BENA435 and 1  $\mu$ M BENA435 mixed with plasmid DNA, dA/dT and dG/dC homopolymers taken at 40  $\mu$ M. Excitation was at 373 nm to show the peak of free BENA435. (D) Fluorescence emission values of 5  $\mu$ M BENA435 titrated with dA/dT and dG/dC homopolymers. Graphs show emission values at 484 nm after excitation at 435 nm. Error bars in (A) and (B) show SEM.

### Structure-activity relationship in the BENA435 series

To get a further insight into how the structural properties of BENA435 contribute to its binding to DNA, we analysed 14 structural analogues present in the compound library. Although several of these compounds are fluorescent *in vivo*, this property went undetected in the initial screen most likely due to the latency period before the appearance of the signal (see below). To evaluate the activity of BENA435-like molecules three tests were used (i) *in vivo*, we incubated human fibroblasts in the presence of the molecules and scored nuclear fluorescence in the microscope; (ii and iii) *in vitro* we looked at the absorption and fluorescence of free molecules before and after addition of plasmid DNA. Table 1 summarizes the results. Cells were observed in inverted epifluorescence microscope using an oil immersion objective and Alexa488/FITC filter. With the exception of BENA435 and analogues **8** and **12**, accurate *in vitro* measurement of the fluorescence intensities was impossible because the emission peaks for the free molecules were too close to that

for the DNA-bound dye. This affected the height of the dye/DNA peaks.

Compounds **1–8** are negative in *in vivo* tests. Compound **1** is also negative in *in vitro* tests. Compounds **2–7** show excitation/emission maxima at wavelengths much lower than those of BENA435. We found that the presence of the methoxy group at the 8-position in the BENA core structure (Figure 1A and Table 1) is necessary for *in vivo* activity of BENA435-like compounds. For instance, compound **8**, which does not stain nuclei *in vivo*, differs from BENA435 solely by the absence of this functionality. Interestingly, however, this compound was fluorescent with DNA *in vitro*, although its fluorescence strength at 468 nm was only 40% of that for BENA435 (Supplementary Data). This suggests that *in vivo* other factors, such as cell-membrane permeability, may be important. It was also observed that molecules containing the 6-*N,N*-dimethyl-propane-1,3-diamino side chain(s) (BENA435, and compounds **10** and **11**) rather than the corresponding 6-*N,N*-dimethyl-ethane-1,2-diamino motif found in compounds **9**, **12**, **13** and **14** displayed a higher

**Table 1.** Summary of properties of 14 BENA435-related molecules

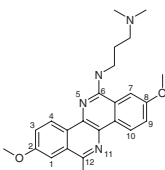
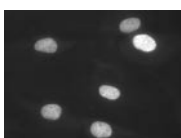
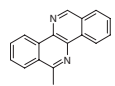
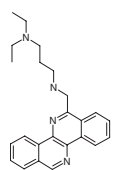
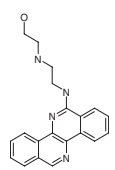
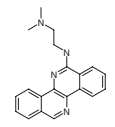
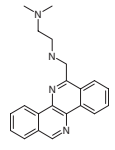
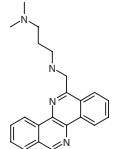
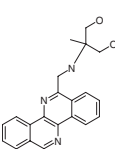
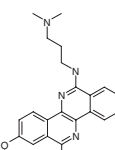
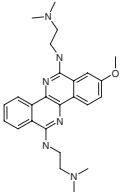

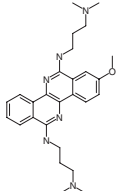
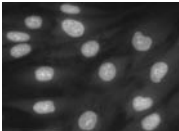
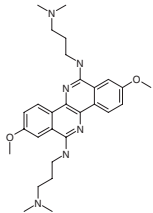
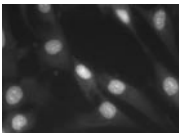
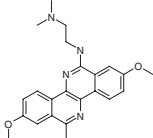

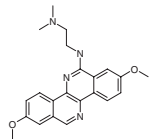
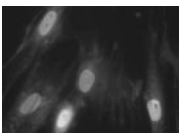
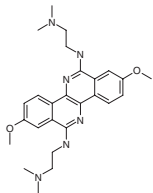
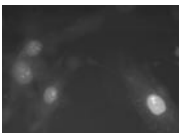
Molecule	Formula MW	Structure	Absorption maxima free/DNA bound dye	Fluorescence maxima free/DNA bound dye	Images of the <i>in vivo</i> nuclear staining <sup>a</sup>
BENA 435	C <sub>24</sub> H <sub>28</sub> N <sub>4</sub> O <sub>2</sub> 404.5		394/435	438/484	 Strong
1	C <sub>17</sub> H <sub>12</sub> N <sub>2</sub> 244.3		ND/ND	ND/ND	—
2	C <sub>24</sub> H <sub>28</sub> N <sub>4</sub> 372.5		360/365	ND/ND	—
3	C <sub>20</sub> H <sub>20</sub> N <sub>4</sub> O 332.4		375/375	ND/ND	—
4	C <sub>20</sub> H <sub>20</sub> N <sub>4</sub> 316.4		370/375	404/ND	—
5	C <sub>21</sub> H <sub>22</sub> N <sub>4</sub> 330.4		365/ND	392/ND	—
6	C <sub>22</sub> H <sub>24</sub> N <sub>4</sub> 344.5		360/365	385/ND	—
7	C <sub>21</sub> H <sub>21</sub> N <sub>3</sub> O <sub>2</sub> 347.4		365/ND	ND/ND	—
8	C <sub>23</sub> H <sub>26</sub> N <sub>4</sub> O 374.5		385/425	427/468	—

Table 1. Continued

Molecule	Formula MW	Structure	Absorption maxima free/DNA bound dye	Fluorescence maxima free/DNA bound dye	Images of the <i>in vivo</i> nuclear staining <sup>a</sup>
9	C <sub>25</sub> H <sub>32</sub> N <sub>6</sub> O 432.6		375/395	468/472	 Weak
10	C <sub>27</sub> H <sub>36</sub> N <sub>6</sub> O 460.6		380/402	478/485	 Moderate/Strong
11	C <sub>28</sub> H <sub>38</sub> N <sub>6</sub> O <sub>2</sub> 490.7		390/405	484/500	 Moderate/Strong
12	C <sub>23</sub> H <sub>26</sub> N <sub>4</sub> O <sub>2</sub> 390.5		390/435	435/475	 Weak
13	C <sub>22</sub> H <sub>24</sub> N <sub>4</sub> O <sub>2</sub> 376.5		390/394	425/407	 Moderate <sup>b</sup>
14	C <sub>26</sub> H <sub>34</sub> N <sub>6</sub> O <sub>2</sub> 462.6		400/400	468/482	 Weak

<sup>a</sup>Staining was defined as 'weak', 'moderate' or 'strong' based on the nuclear signal/background ratio.

<sup>b</sup>In the presence of these molecules nuclei did not fluoresce initially when visualized in the Alexa488/FITC filter, but became noticeable after a short (10 s) pre-illumination with UV light (DAPI/Hoechst filter; Omega XF03). ND, not determined (impossible to measure).

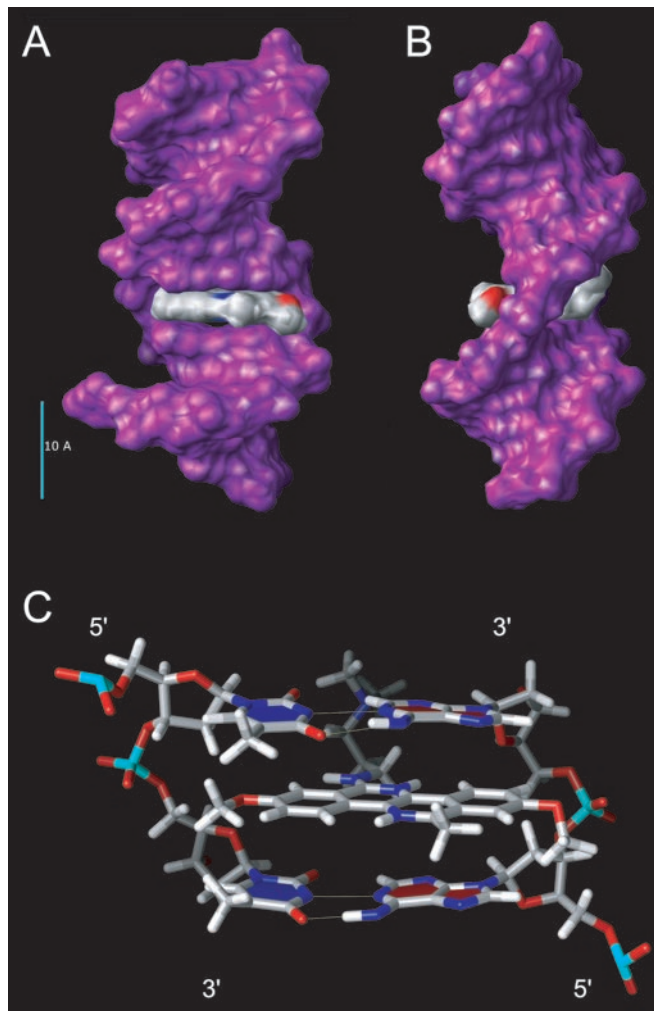
signal-to-background ratio in *in vivo* experiments. The presence of this longer chain may contribute to improved cell permeability, as illustrated by the difference in *in vivo* nuclear staining between molecules **9** and **10**.

Finally, compound **13** which lacks the methyl group at position 12, becomes fluorescent in cell nuclei using the green (Alexa488/FITC) filter after it has been briefly pre-flashed (10 s) using a UV filter (Omega XF03). These results indicate that molecule **13** is excited at shorter wavelengths

than BENA435. Indeed, *in vitro* in the presence of dsDNA its absorption and emission maxima were 394/407.

The above observations suggest that the structure of BENA435 is, relatively speaking, already optimized, since a number of minor modifications have a deleterious effect on either its permeability, its interaction with DNA or its fluorescent properties. In this context, although the C-12 methyl group is not crucial to 'activity', it is important for the red shift in the emission of DNA-bound BENA435 type





**Figure 4.** Putative model of BENA435 intercalated between two pairs of dA/dT bases. (A) View from the major groove side. (B) Side view (major groove on the left-hand side). (C) BENA435 stacked between two dA/dT pairs of bases. Yellow lines represent H-bonds.

molecules. The cationic side chain(s) seem(s) to be important for either permeability or binding to DNA.

#### Molecular modelling of BENA435 binding to DNA

Modelling of BENA435 structure predicts a flat rigid heterocyclic core (Figure 1B) with a flexible positively charged side chain. As hydrodynamic studies suggested that BENA435 intercalates between DNA strands, we propose a putative model of BENA435 inserted into DNA structure. For this we used the ArgusLab 4.0.1 software and the atomic coordinates of a dsDNA dodecamer 5'-D(CGCGAATTCGCG)-3' complexed with an Acridine-peptide drug. For docking we used the ArgusLab scoring function AScore and a grid encompassing the whole dodecamer. The lowest energy conformation ( $-4.00$  kcal/mol), shown in Figure 4, represents BENA435 stacked between two pairs of nucleotides (AT/AT). Similar results were obtained using a genetic algorithm scoring function or two pairs of GC nucleotides (Supplementary Data).

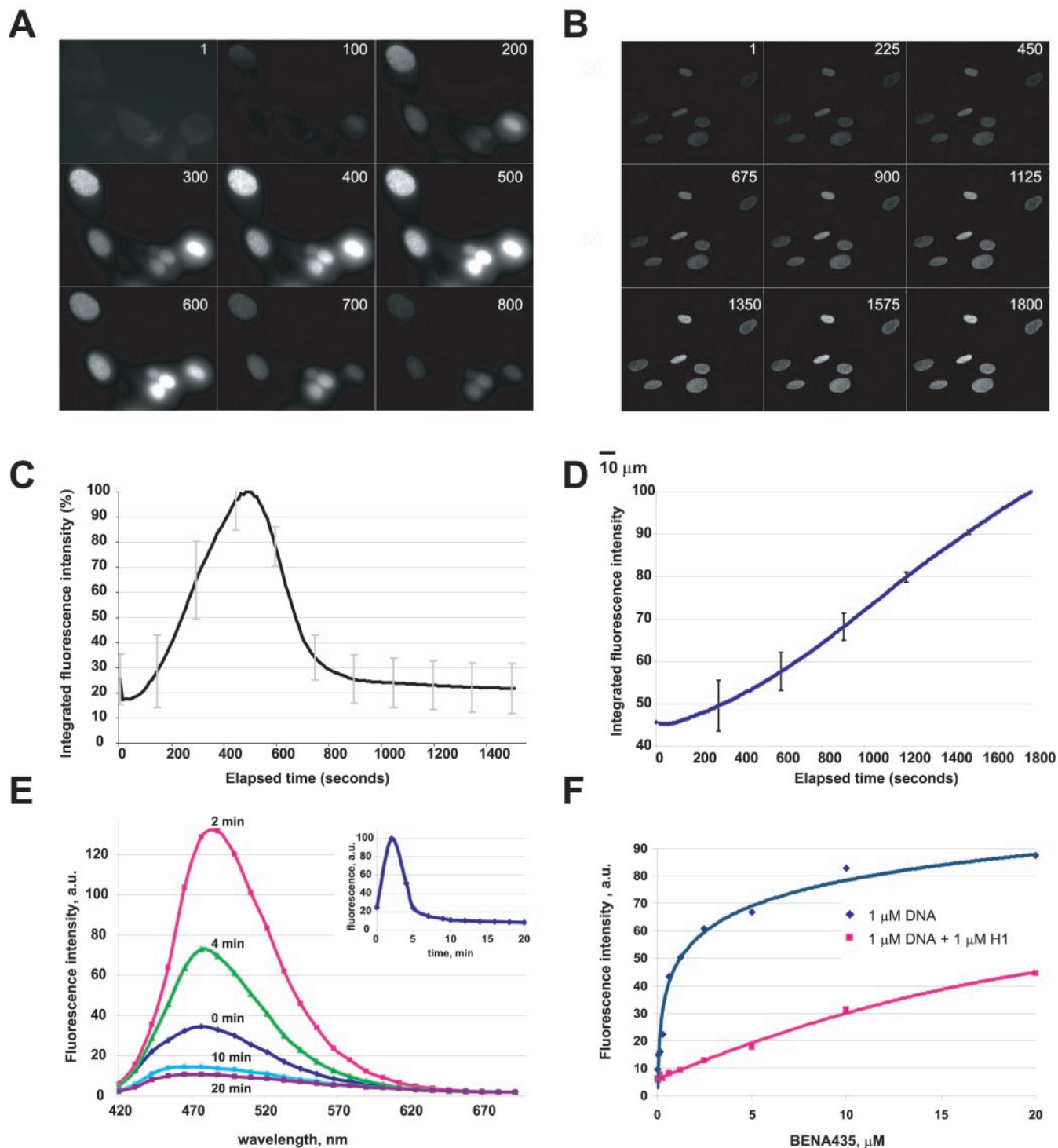
#### BENA435 is activated by light

Initial *in vivo* observations of BENA435-treated cells showed that the green nuclear staining appeared after a latency period of 10–20 s (depending on concentration), suggesting a photoactivation phenomenon. To quantify this effect, live mouse fibroblasts were incubated in the presence of  $5 \mu\text{M}$  BENA435 and time-lapse video microscopy was used to film the cells. Nuclear fluorescence develops slowly in the nuclei of cells treated with BENA435 and illuminated continuously using a standard Alexa488/FITC filter set (475AF40, 535AF45) (Figure 5A). Fluorescence peaked after 8 min of illumination and then started to fade (Figure 5C), most likely reflecting the ‘bleaching’ of BENA435. The photoactivation concerned only the cells in the illuminated field, as nuclei of cells immediately outside of the illuminated field remained imperceptible (non-fluorescent, data not shown). Theoretically, it was possible that photoactivation was due to a chemical modification of the structure of BENA435 catalysed by living cells. To test this possibility we stained nuclei of fixed cells with BENA435 and measured nuclear fluorescence during a continuous 30 min illumination. Figure 5B and D show that in fixed cells BENA435/DNA fluorescence increase linearly over a long period of time. Nuclei of cells located immediately outside of the illuminated field remained dim (data not shown). Photoactivation did not happen when BENA435 was mixed with DNA at different dye/bp ratios and illuminated in the microscope as described above (Supplementary Data). Hypothetically, it was possible that the increase in fluorescence as seen in a band pass Alexa488/FITC filter represented a shift in the wavelength of emission over time. To determine whether this was occurring we recorded spectra of BENA435 emission in the nuclei of live cells using a confocal microscope. Figure 5E shows that the emission spectrum of DNA-bound BENA435 does not change considerably over time when excited at 405 nm. Similar results were obtained using excitation at 458 nm (data not shown), meaning that the change in fluorescence intensities does not result from a major change in the emission wavelength.

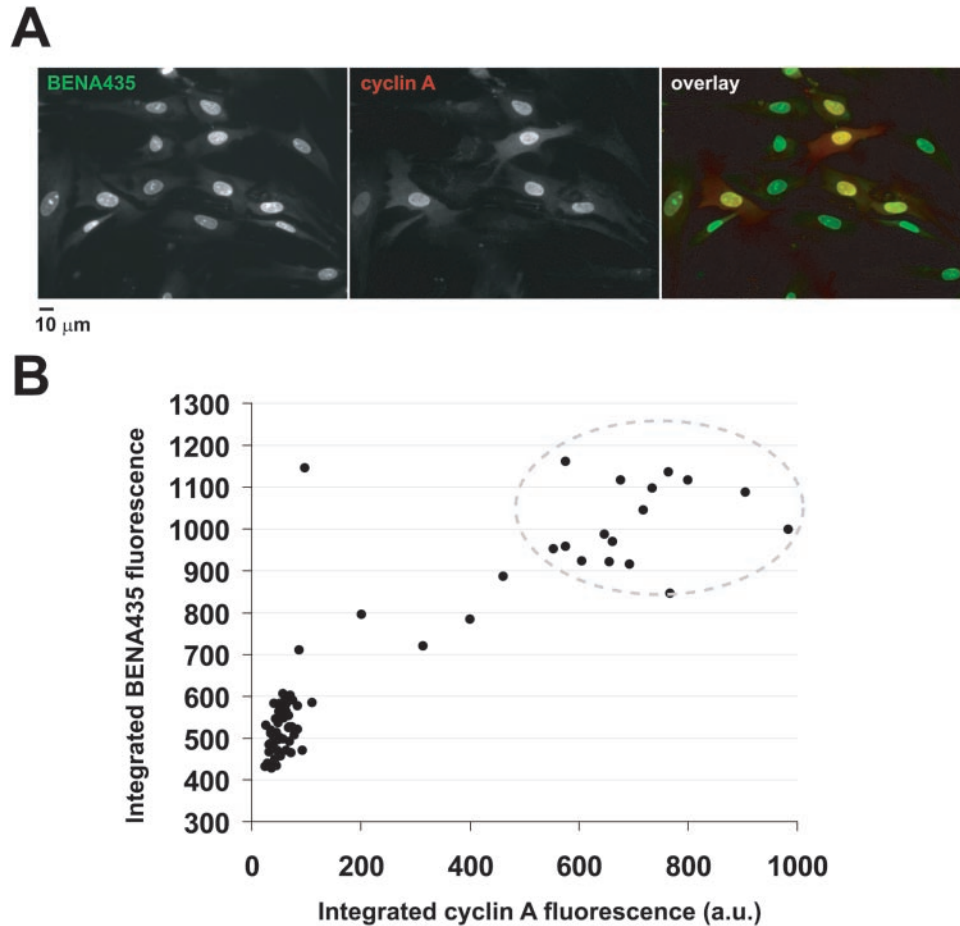
As competition with chromatin proteins such as histones and HGM1 has been shown to affect binding of both external binders (23–25) and intercalating small molecules (26–28), we asked ourselves whether BENA435/DNA fluorescence was affected by the presence of histones. Titration of  $1 \mu\text{M}$  plasmid DNA with BENA435 in the absence or presence of  $1 \mu\text{M}$  human histone 1 (H1) showed that H1 significantly affected the fluorescence of BENA435 (Figure 5F). At the same time free BENA435 fluorescence (excited at 391 nm) was not quenched by H1 (data not shown). We conclude therefore that BENA435 fluorescence in cells is activated by light, and this photoactivation most likely depends on DNA being in complex with proteins which are not affected by methanol fixation (Discussion).

#### BENA435 allows an easy DNA quantification in cells

Some of the BENA435-stained nuclei appeared brighter than others (Figure 1C and Figure 5A and B) suggesting that fluorescence intensities may be proportional to their DNA content and correspondingly reflect their cell cycle status, as was shown for other DNA probes, e.g. for PicoGreen and SYBR Green I. Probing directly DNA content in live cells



**Figure 5.** Photoactivation of BENA435 in live and fixed cells. (A) Panel of images showing photoactivation of DNA-bound BENA435 in live cells. Fibroblasts incubated with  $5 \mu\text{M}$  BENA435 and illuminated using an Alexa488/FITC develop a bright nuclear signal which reaches a plateau after 8 min. Numbers correspond to time points (s). (B) Panel of images showing activation of BENA435 in fixed cells. Methanol-fixed primary human fibroblasts were stained with BENA435 as described in Materials and Methods and images were taken at 10 s intervals during a continuous 30 min illumination using a 100 W mercury lamp. Numbers correspond to time points. In a representative nucleus average pixel values were 512 in the plane (1) and 1434 in the plane (1800). (C) Quantification of the fluorescence shown in (A). Graph shows average nuclear fluorescence over 26 min. (D) Quantification of the fluorescence shown in (B). Graph shows average nuclear fluorescence over 30 min. All of the nuclei shown in (B) were used for quantification. (E) Representative emission spectra of the nucleus in a live 3T3 cell, incubated in the presence of  $5 \mu\text{M}$  BENA435 and excited at 405 nm. Curves correspond to scans performed at the shown time points. Insert in the upper right corner shows activation of BENA435 measured in the nucleus in the course of experiment [similar to (C)]. (F) Fluorescence values of different amounts of BENA435 mixed with  $1 \mu\text{M}$  plasmid DNA in the absence or presence of  $1 \mu\text{M}$  histone 1. Emission at 484 nm after excitation at 435 nm. Lines were drawn through the points to guide the eye and do not represent a fitting to any equation. Error bars in (C) and (D) correspond to SD.



**Figure 6.** BENA435 nuclear fluorescence reflects cell cycle stage. (A) Images show the same representative microscopic field with methanol-fixed fibroblasts stained using anti-cyclin A antibodies and counterstained by BENA435. Images were acquired using a 20 $\times$  objective. (B) Quantification of the nuclear fluorescence in cells stained with BENA435 and anti-cyclin A antibodies [experiment shown in (A)]. Dots represent 81 nuclei measured in 6 different randomly chosen microscopic fields. Region in the upper right corner surrounds strongly cyclin A-positive cells.

already stained by BENA435 would necessitate using another dsDNA-binding dye. Such a double staining carried the risk of a possible competition for binding sites and/or unpredictable effects on fluorescence. Therefore we decided to compare the integrated total fluorescence of BENA435-stained nuclei in fixed cells with a known cell cycle protein marker. We fixed primary human fibroblasts with methanol, performed indirect immunofluorescence with anti-cyclin A antibodies, followed by Alexa 568-labelled secondary antibodies and counterstained nuclei with BENA435. Cyclin A accumulates in cells beginning at the S phase and throughout the G2 cell cycle phase, and unlike cyclin B, is practically all nuclear [reviewed in (29)]. This fact facilitates the correlation of BENA435/DNA fluorescence with that of cyclin A. Indeed, we found that cells negative for cyclin A have significantly lower BENA435 fluorescence in the nucleus (Figure 6A). Moreover, we observed a direct correlation of the BENA435 fluorescence with that of cyclin A in cyclin A-positive cells (Figure 6B). Of note is that strongly cyclin A-positive nuclei (Figure 6B, dots in the upper right corner showed by oval) contain approximately twice as much BENA435-fluorescence as cyclin A-negative nuclei. This correlates well with 2N and 4N DNA content expected to be

found in G1 and G2 cells, respectively. These results show that BENA435 allows an easy quantification of nuclear DNA content, reflecting the cell cycle stage.

## DISCUSSION

### Fluorescent properties of BENA435

The absorption/emission characteristics displayed by BENA435 make this compound highly attractive as a reagent for fluorescence staining of DNA. The Acridine homodimer and certain low-affinity DNA-binding SYTO dyes have similar absorption/emission maxima. However, unlike BENA435, the acridine dye is cell-membrane non-permeant (1,30), and the SYTO dyes are known to be non-selective DNA staining reagents, staining RNA *in vivo*, as well other structures including mitochondria (1). This is not surprising, as practically all DNA dyes also bind RNA and/or ssDNA to some extent. For example, the thiazole orange homodimer (TOTO) and ethidium bromide interact *in vitro* with dsDNA and ssDNA with similar affinity (31). Our *in vitro* and *in vivo* results suggest that BENA435 fluoresces preferentially when bound to dsDNA rather than to RNA. The difference was most

pronounced at low dye/b(p) ratios, with BENA435/DNA fluorescence at least 6-fold higher than that for the BENA435/RNA complex. Moreover, when we titrated 5  $\mu$ M BENA435 with increasing amounts of DNA and RNA we found that DNA was saturated with dye at  $\sim$ 30 bp/dye, while RNA could not be saturated at even a 250 b/dye ratio (Supplementary Data). On the other hand, the fact that at increasing dye/b(bp) ratios the difference in BENA435 fluorescence bound to DNA or RNA was smaller (Figure 2A) could mean that BENA435 may also interact with nucleic acids through other than intercalation mechanism.

Of note, when compared with an intercalating DNA probe ethidium bromide, BENA435 shows surprisingly similar selectivity toward DNA over RNA (Supplementary Data). The quantum yield of BENA435 when bound to DNA (13.8%) is also very close to that reported for ethidium bromide, (15%) (32). *In vivo*, and on fixed cells, BENA435 stains only nuclei and not the cytoplasm where the bulk of RNA is localized. This suggests that the concentrations of BENA435 and the conditions used for staining are optimal for efficient discrimination between dsDNA and RNA.

We found that BENA435 fluoresces preferentially when bound to dA/dT rather than to dG/dC tracts. This differs from YO, which, when complexed with DNA, behaves in the opposite way, showing a net increase in quantum yield when complexed with dG/dC homopolymers rather than with dA/dT homopolymers (22). Some other intercalators like SYBR Green I (5) and ciprofloxacin (33) display selectivity which is similar to BENA435's. However, the difference in the fluorescence of these dyes bound to dA/dT and dG/dC homopolymers is much less pronounced than in the case of BENA435. The extent of this difference cannot be explained by the lack of binding to dG/dC tracts, as the peak of fluorescence of free BENA435 practically disappears as well. Also, absorption experiments show that BENA435 binds similarly well to dG/dC and dA/dT tracts (Supplementary Data). All this suggests that BENA435 can bind to, but interacts differently with, dA/dT and dG/dC pairs of nucleotides. The observed quenching effect by dG/dC tracts could come from the low oxidation potential reported for guanine or from the electron transfer between BENA435 and guanine residues as was reported for other fluorescent intercalating molecules (22,33,34).

### Structure function relationship

Depending on their structure, fused poly(hetero)aromatic molecules can bind to DNA through intercalation (2), or minor/major groove binding [reviewed in (35)]. BENA435 is a neutral aza analogue of the alkaloid fagaronine (15), which is known to intercalate into DNA, but which was not reported to be a fluorescent DNA marker. The binding of BENA435 to DNA is probably helped by the presence of the dialkylamine containing side chain which is positively charged at physiological pH. As was shown for other cationic dyes (5,36,37), *in vitro* salt significantly affected the fluorescence of BENA435/DNA (Supplementary Data). These data support the idea that the cationic side chain participates in the binding of dye to the ds helix. Hypothetically, the side chain could interact with the negative chargers on the backbone phosphate residues.

The proposed model of BENA435 bound to the dsDNA fits experimental data suggesting that at low dye/bp ratio BENA435 can intercalate between base pairs. We cannot however exclude that at higher concentrations of BENA435 the dye may also show some external binding, as is the case for some other DNA probes (5). Indeed, modelling with a DNA structure without a space between base pairs (where BENA435 could intercalate) suggests that BENA435 could easily fit into the minor groove (data not shown).

In our phenotypical screen we have only found BENA435 and none of six BENA-related compounds (9–14) listed in Table 1 which were later shown to stain nuclei *in vivo*. This is not surprising, because of these six molecules some (like 9, 12, 14) show weak activity *in vivo*, and one more fluoresces at wavelengths too short to be efficiently seen in the Alexa488/FITC filter (13). Finally, the short observation time during screening may not have allowed the staining to develop (see below). With exception of molecules 8 (inactive *in vivo*) and 12 (weakly active *in vivo*) all other BENA435-like molecules have relatively close peaks of emission of the free and DNA-bound dye, possibly contributing to higher background staining. Therefore, out of all molecules studied BENA435 structure is most optimised for DNA detection in cells using a standard green fluorescence filter.

### Photoactivation

As we have shown, photoactivation of BENA435 does occur in fixed cells, indicating that the molecule did not undergo any structural modifications *in vivo*. Moreover, the spectra of emission of BENA435 *in vitro* and in cells are practically identical. On the other hand, photoactivation is not observed with pure plasmid DNA. It is thus likely that this phenomenon is dependent on DNA being associated with proteins (chromatin). Indeed, both minor groove-binding probes like DAPI or intercalating molecules such as ethidium bromide or chromomycin A3 were shown to disrupt the nucleosome and/or prevent its assembly. At least two different mechanisms may be responsible for this effect. Externally binding dyes may compete for the dA/dT rich binding sites with histones or other chromatin proteins, or inhibit DNA movement/flexibility, which is followed by reduced histone–DNA contacts within the minor groove (23). Intercalators can unwind the DNA helix, lengthen and stiffen it [(38) and references therein]. Importantly, we have shown that *in vitro* DNA-dependent fluorescence of BENA435 is inhibited by H1. This suggests that the observed in cells photoactivation of BENA435 may in fact reflect a slow binding to DNA with concomitant displacing of histones and/or other chromatin proteins from their association with DNA. This hypothesis is corroborated by the fact that, unlike in live cells, on fixed cells BENA435 was immediately fluorescent, although its intensity further increased over the time. This can be explained by the fact that fixation partially denatures chromatin proteins, leaving DNA more accessible to BENA435 than it is the case in live cells. Finally, it remains to show why the binding of BENA435 to DNA is enhanced by light.

### SUPPLEMENTARY DATA

Supplementary Data are available at NAR Online.

## ACKNOWLEDGEMENTS

We are grateful to colleagues from the BioPuces Laboratory, CEA-Grenoble, and to C.Allain (Collège de France) for access to and help with fluorimetry. We thank A. Imberty, B. Laudet and R. Prudent for help with molecular modelling, D. Grunwald for assistance with confocal analysis, C. Ebel for help with viscometry. For comments on the manuscript and suggestions we thank F. Pirolet, V. Rybin and M. Balakirev. Research in the group of A.P. is funded by the Avenir grant of Inserm, ACI BCMS of the French Research Ministry (project BCM0210), equipment grant of the 'La Ligue contre le Cancer' (Comité de l'Isère), equipment grant 'Emergence 2004' of the Department de Rhône-Alpes and equipment grant of the 'Association pour la Recherche sur le Cancer' (project 7833). Funding to pay the Open Access publication charges for this article was provided by the ACI grant of the French Research Ministry.

*Conflict of interest statement.* None declared.

## REFERENCES

- Haugland,R.P. (ed.) (2002) Nucleic Acid Detection and Genomics Technology (Chapter 8). 9th edn. Molecular Probes, Inc., Eugene, OR.
- Lerman,L.S. (1961) Structural considerations in the interaction of DNA and acridines. *J. Mol. Biol.*, **3**, 18–30.
- Kopka,M.L., Yoon,C., Goodsell,D., Pjura,P. and Dickerson,R.E. (1985) The molecular origin of DNA-drug specificity in netropsin and distamycin. *Proc. Natl Acad. Sci. USA*, **82**, 1376–1380.
- Kubista,M., Akerman,B. and Norden,B. (1987) Characterization of interaction between DNA and 4',6-diamidino-2-phenylindole by optical spectroscopy. *Biochemistry*, **26**, 4545–4553.
- Zipper,H., Brunner,H., Bernhagen,J. and Vitzthum,F. (2004) Investigations on DNA intercalation and surface binding by SYBR Green I, its structure determination and methodological implications. *Nucleic Acids Res.*, **32**, e103.
- Alexander,P. and Moroson,H. (1962) Cross-linking of deoxyribonucleic acid to protein following ultra-violet irradiation different cells. *Nature*, **194**, 882–883.
- Pfeifer,G.P., You,Y.H. and Besaratinia,A. (2005) Mutations induced by ultraviolet light. *Mutat. Res.*, **571**, 19–31.
- Palitti,F. (2004) Mechanisms of formation of chromosomal aberrations: insights from studies with DNA repair-deficient cells. *Cytogenet. Genome Res.*, **104**, 95–99.
- Kulms,D. and Schwarz,T. (2002) Molecular mechanisms involved in UV-induced apoptotic cell death. *Skin Pharmacol. Appl. Skin Physiol.*, **15**, 342–347.
- Tramier,M., Kemnitz,K., Durieux,C., Coppey,J., Denjean,P., Pansu,R.B. and Coppey-Moisson,M. (2000) Restrained torsional dynamics of nuclear DNA in living proliferative mammalian cells. *Biophys. J.*, **78**, 2614–2627.
- Bisagni,E., Landras,C., Thiroit,S. and Huel,C. (1996) A convenient way to dibenzo[c,h]-1,5-naphthyridines (11-aza-benzo[c] phenanthridines). *Tetrahedron*, **52**, 10427–10440.
- Miller,L. and Daniel,J.C. (1977) Comparison of *in vivo* and *in vitro* ribosomal RNA synthesis in nucleolar mutants of *Xenopus laevis*. *In Vitro*, **13**, 557–563.
- IUPAC Commission on Photochemistry (1986), EPA Newsletter of November. 21–29.
- Muller,W. and Crothers,D.M. (1968) Studies of the binding of actinomycin and related compounds to DNA. *J. Mol. Biol.*, **35**, 251–290.
- Sadowski,J. (2004) 3D structure generation. Gasteiger,J. (ed.), *Handbook of Chemoinformatics—From Data to Knowledge*. Wiley-VCH, Weinheim, pp. 231–261.
- Thompson,M.A. (2004) ArgusLab 4.0.1. Planaria Software LLC, Seattle, WA.
- Morris,G.M., Goodsell,D.S., Halliday,R.S., Huey,R., Hart,W.E., Belew,R.K. and Olson,A.J. (1998) Automated docking using a Lamarckian Genetic Algorithm and Empirical Binding Free Energy Function. *J. Comput. Chem.*, **19**, 1639–1662.
- Malinina,L., Soler-Lopez,M., Aymami,J. and Subirana,J.A. (2002) Intercalation of an acridine-peptide drug in an AA/TT base step in the crystal structure of [d(CGCGAATTCGCG)]<sub>2</sub> with six duplexes and seven Mg(2+) ions in the asymmetric unit. *Biochemistry*, **41**, 9341–9348.
- Pettersen,E.F., Goddard,T.D., Huang,C.C., Couch,G.S., Greenblatt,D.M., Meng,E.C. and Ferrin,T.E. (2004) UCSF Chimera—a visualization system for exploratory research and analysis. *J. Comput. Chem.*, **25**, 1605–1612.
- Suh,D. and Chaires,J.B. (1995) Criteria for the mode of binding of DNA binding agents. *Bioorg. Med. Chem.*, **3**, 723–728.
- Lakowicz,J.R. (1991) *Fluorescence Quenching: Theory and Applications*. 2nd edn. Kluwer Academic/Plenum, New York, NY.
- Larsson,A., Carlsson,C. and Jonsson,M. (1995) Characterization of the binding of YO to [poly(dA-dT)]<sub>2</sub> and [poly(dG-dC)]<sub>2</sub>, and of the fluorescent properties of YO and YOYO complexed with the polynucleotides and double-stranded DNA. *Biopolymers*, **36**, 153–167.
- Fitzgerald,D.J. and Anderson,J.N. (1999) Selective nucleosome disruption by drugs that bind in the minor groove of DNA. *J. Biol. Chem.*, **274**, 27128–27138.
- Churchill,M.E. and Suzuki,M. (1989) 'SPKK' motifs prefer to bind to DNA at A/T-rich sites. *EMBO J.*, **8**, 4189–4195.
- Reeves,R. and Nissen,M.S. (1990) The A.T-DNA-binding domain of mammalian high mobility group I chromosomal proteins. A novel peptide motif for recognizing DNA structure. *J. Biol. Chem.*, **265**, 8573–8582.
- McMurray,C.T., Small,E.W. and van Holde,K.E. (1991) Binding of ethidium to the nucleosome core particle. 2. Internal and external binding modes. *Biochemistry*, **30**, 5644–5652.
- Mir,M.A. and Dasgupta,D. (2001) Association of the anticancer antibiotic chromomycin A(3) with the nucleosome: role of core histone tail domains in the binding process. *Biochemistry*, **40**, 11578–11585.
- Mir,M.A., Das,S. and Dasgupta,D. (2004) N-terminal tail domains of core histones in nucleosome block the access of anticancer drugs, mithramycin and daunomycin, to the nucleosomal DNA. *Biophys. Chem.*, **109**, 121–135.
- Pines,J. and Hunter,T. (1992) Cyclins A and B1 in the human cell cycle. *Ciba Found Symp.*, **170**, 187–196; discussion 196–204.
- Le Pecq,J.B., Le Bret,M., Barbet,J. and Roques,B. (1975) DNA polyintercalating drugs: DNA binding of diacridine derivatives. *Proc. Natl Acad. Sci. USA*, **72**, 2915–2919.
- Rye,H.S. and Glazer,A.N. (1995) Interaction of dimeric intercalating dyes with single-stranded DNA. *Nucleic Acids Res.*, **23**, 1215–1222.
- Le Pecq,J.B. (1971) Use of ethidium bromide for separation and determination of nucleic acids of various conformational forms and measurement of their associated enzymes. *Methods Biochem. Anal.*, **20**, 41–86.
- Vilfan,I.D., Drevensek,P., Turel,I. and Poklar Ulrih,N. (2003) Characterization of ciprofloxacin binding to the linear single- and double-stranded DNA. *Biochim. Biophys. Acta*, **1628**, 111–122.
- Ihmels,H., Faulhaber,K., Wissel,K., Viola,G. and Vedaldi,D. (2003) 6-Aminoacridizinium bromide: a fluorescence probe which lights up in AT-rich regions of DNA. *Org. Biomol. Chem.*, **1**, 2999–3001.
- Johnson,D.S. and Boger,D.L. (1996) DNA binding agents. Murakami,Y. (ed.), *Comprehensive Supramolecular Chemistry*. Elsevier, Oxford, pp. 73–176.
- Blackburn,G.M. and Gait,M.J. (1996) *Nucleic acids in chemistry and biology*. (ed.), 2nd edn. Oxford University Press, Oxford, pp. 329–370.
- Eriksson,M., Karlsson,H.J., Westman,G. and Akerman,B. (2003) Groove-binding unsymmetrical cyanine dyes for staining of DNA: dissociation rates in free solution and electrophoresis gels. *Nucleic Acids Res.*, **31**, 6235–6242.
- McMurray,C.T. and van Holde,K.E. (1986) Binding of ethidium bromide causes dissociation of the nucleosome core particle. *Proc. Natl Acad. Sci. USA*, **83**, 8472–8476.